


CLINICAL RESEARCH

Research funding by the ACVS Foundation

Comparison of three-dimensional printed patient-specific guides versus freehand approach for radial osteotomies in normal dogs: Ex vivo model

Adam Townsend DVM¹ | Julien Guevar DVM, MVM, DECVN, MRCVS² |
 Bill Oxley MA, VetMB, DSAS(Orth)³ | Scott Hetzel MS⁴ |
 Jason Bleedorn DVM, MS, DACVS-SA^{1,5} 

¹Department of Surgical Sciences and Comparative Orthopedic Research Laboratory, School of Veterinary Medicine, University of Wisconsin-Madison, Madison, Wisconsin, USA

²Division of Surgery, Department of Clinical Veterinary Medicine, Vetsuisse Faculty, University of Bern, Bern, Switzerland

³Vet 3D, Coventry, UK

⁴Department of Biostatistics and Medical Informatics, University of Wisconsin-Madison, Madison, Wisconsin, USA

⁵Veterinary Clinical Sciences, Colorado State University, Fort Collins, Colorado, USA

Correspondence

Jason Bleedorn, Department of Surgical Sciences and Comparative Orthopedic Research Laboratory, School of Veterinary Medicine, University of Wisconsin-Madison, Madison, WI, USA.
 Email: j.bleedorn@colostate.edu

Funding information

American College of Veterinary Surgeons Foundation; Companion Animal Fund-UW-Madison

Abstract

Objective: To compare the accuracy of three-dimensional (3D) printed patient-specific guide (PSG) with a freehand (FH) approach for radial osteotomies in ex vivo normal dogs.

Study design: Experimental study.

Animals: Twenty four ex vivo thoracic limb pairs from normal beagle dogs.

Methods: Computed tomography (CT) images were collected preoperatively and postoperatively. Three osteotomies tested ($n = 8/\text{group}$) were: (1) uniplanar 30° frontal plane wedge osteotomy, (2) oblique plane (30° frontal, 15° sagittal) wedge osteotomy, and (3) single oblique plane osteotomy (SOO, 30° frontal, 15° sagittal, and 30° external). Limb pairs were randomized to a 3D PSG or FH approach. The resultant osteotomies were compared with virtual target osteotomies by surface shape-matching postoperative to the preoperative radii.

Results: The mean \pm standard deviation osteotomy angle deviation for all 3D PSG osteotomies ($2.8 \pm 2.8^\circ$, range 0.11–14.1°) was less than for the FH osteotomies ($6.4 \pm 6.0^\circ$, range 0.03–29.7°). No differences were found for osteotomy location in any group. In total, 84% of 3D PSG osteotomies were within 5° deviance from the target compared to 50% of freehand osteotomies.

Conclusion: Three-dimensional PSG improved FH accuracy of osteotomy angle in select planes and the most complex osteotomy orientation in a normal ex vivo radial model.

Clinical significance: Three-dimensional PSGs provided more consistent accuracy, which was most notable in complex radial osteotomies. Future work

Abbreviations: 3D, three-dimensional; CAD, computer-aided design; CORA, center of rotation and angulation; CT, computed tomography; DICOM, Digital Imaging and Communications in Medicine; FH, freehand; PSG, patient-specific guide; SLA, stereolithographic; SOO, single oblique plane osteotomy.

This is an open access article under the terms of the [Creative Commons Attribution-NonCommercial-NoDerivs](https://creativecommons.org/licenses/by-nc-nd/4.0/) License, which permits use and distribution in any medium, provided the original work is properly cited, the use is non-commercial and no modifications or adaptations are made.

© 2023 The Authors. *Veterinary Surgery* published by Wiley Periodicals LLC on behalf of American College of Veterinary Surgeons.

is needed to investigate guided osteotomies in dogs with antebrachial bone deformities.

1 | INTRODUCTION

Limb deformities are complex orthopedic conditions in dogs that may result in substantial pain and disability if untreated. The radius and ulna are the most common bones affected in dogs, and usually manifest in asynchronous growth of these paired bones.¹ Deformity may result in tremendous angulation and rotational malalignment, as well as carpal and elbow joint incongruity.¹ Surgical correction requires accurate quantification of the deformity, and subsequent execution of this plan in the operating room.

Planning has historically been performed with a center of rotation of angulation (CORA) methodology using two-dimensional radiography² and more recently applied to computed tomography (CT) imaging.³ A majority of antebrachial deformity cases contain malalignment in the frontal, sagittal, and axial planes which can be quantified independently. However, current methods still resolve these 3D structures into 2D images for quantification using 3D multiplanar and volume reconstruction approaches.^{2,4} Transferring these detailed 3D plans to guide operative surgery is an additional fundamental obstacle.

Computer-aided design (CAD) for 3D planning and printing is an established technology in medical fields.⁵ Widespread applications exist in human orthopedic, maxillofacial, and spinal surgery, among others, but relatively little comparative information in veterinary medicine and surgery is available. Orthopedics and bone deformity correction is an obvious target due to ease of segmentation of bone from CT data due to its high Hounsfield units, allowing for automated and efficient thresholding tools. Furthermore, 3D volume data can be used to print bone models for surgical rehearsal, perform computerized virtual correction based on the plan, and print custom patient-specific guides (PSGs) for use in sterile surgery. Accurate outcomes have been reported in deformity correction of the femur⁶ and antebrachium,^{7,8} as well as implant placement in spine and craniomaxillofacial applications.^{9,10}

Despite successful clinical outcomes using 3D PSGs in clinical veterinary cases, more work is needed from an orthopedic science perspective to robustly examine this approach.¹¹ We lack specific indications and locations for use to justify the time, cost, and expertise needed for 3D planning and guide use. A consistent workflow for 3D

planning to include correction target magnitude for deformity is needed. Finally, best practice guidelines for design approaches, materials, and manufacturing have not been established.

The primary objective of this study was to compare the accuracy and reliability of radial osteotomies performed using 3D PSGs versus a freehand (FH) approach. We tested three osteotomies of increasing complexity on normal ex vivo canine thoracic limbs. Computed tomography was performed preoperatively for planning and guide design, and postoperatively for osteotomy assessment. We hypothesized that 3D PSG osteotomy would be more accurate in achieving an osteotomy within 5° of the intended target than a FH osteotomy in a canine antebrachium model.

2 | METHODS

2.1 | Study design

An ex vivo method-comparison study between 3D PSG and FH corrective osteotomy of the distal radius was performed.

2.2 | Specimen collection and grouping

Twenty-four pairs of clinically normal cadaveric forelimbs were collected from beagle dogs euthanized for reasons unrelated to this study. The limb pairs were randomly assigned using a spreadsheet function (random, roundup, rank; Microsoft Excel) to one of three groups (n = 8 per group). An a priori power analysis determined that eight limbs in a paired design and expecting a clinically relevant mean paired difference of 5° (SD = 3) between freehand and guided methods would achieve 97% power with a paired *t*-test at a 5% significance level. Group 1 was a uniplanar 30° frontal plane wedge osteotomy. Group 2 was an oblique plane (30° frontal plane, 15° sagittal plane) wedge osteotomy. Group 3 was a torsion-angulation osteotomy (30° frontal plane, 15° sagittal plane, and 30° external torsion) using a single oblique plane osteotomy¹² (SOO). Right or left limb pairs were randomly assigned to treatment using 3D PSG or FH approach and treated in ordinal fashion of increasing complexity.

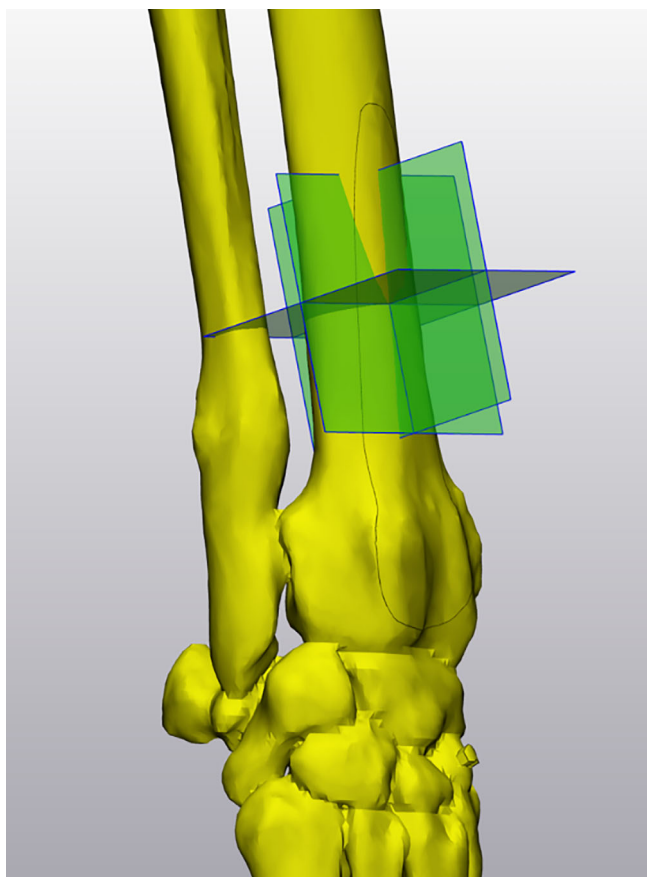


FIGURE 1 Oblique view of the 3D volumetric reconstructions of a right forelimb with the neutral frontal, sagittal, and axial planes defined.

2.3 | Three-dimensional planning

Limb pairs were disarticulated and frozen with the elbow and carpus in full extension. A CT scan of both entire forelimbs was performed with a 64-slice helical scanner (GE Lightspeed VCT, Chicago, Illinois). Transverse 0.625 mm slices with 50% overlap were obtained using a high-frequency bone algorithm. Digital imaging and communications in medicine (DICOM) images were imported into 3D modeling software (Mimics version 22; Materialize, Leuven Belgium) and segmented using thresholding (Hounsfield limits 226–2554), region growing, and editing tools to create a 3D triangular surface model (mesh) of each forelimb. Models were exported to 3D design software (3-Matic, version 14, Materialize, Leuven Belgium) for 3D planning and guide design. The neutral frontal, sagittal, and axial planes were individually defined for each limb based on humeral transcondylar orientation and used to define the object coordinate system (Figure 1). These reference planes and coordinate system were used for standardizing guide design and postoperative assessment.

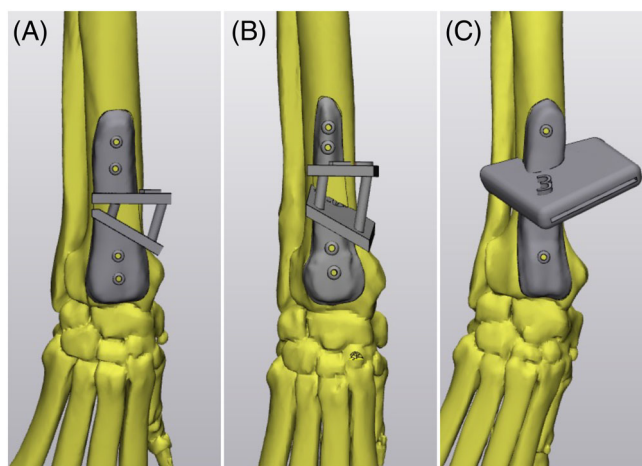


FIGURE 2 Representative images of the osteotomy guides on the right forelimb of group 1 (A) group 2 (B) and group 3 (C). All guides were exported as .STL files and 3D printed on a stereolithographic (SLA) printer using clear resin.

The osteotomy was located at the distal 25% of the radial length in all groups. For groups 1 and 2, a transverse plane was created parallel to the axial reference plane to represent the proximal osteotomy. A duplicate osteotomy plane was created and manipulated for the distal osteotomy. For group 1, the distal cut plane was rotated 30° in the frontal plane, and moved distally along the object coordinate system until the two cut planes met at the lateral cortex of the radius to create a medially based closing wedge. For group 2, the distal osteotomy plane was rotated 30° in the frontal plane, followed by 15° in the sagittal plane, then moved distally along the object coordinate system until the two cut planes met at the caudolateral cortex of the radius to create a craniomedial oblique plane closing wedge. For group 3, the single osteotomy plane was rotated 30° in the frontal plane, then 15° in the sagittal plane, and finally rotated 30° in the axial plane about the object coordinate system for a single oblique plane osteotomy. Images showing virtual osteotomy position were saved and exported for reference in surgery.

2.4 | Computer-aided guide design and 3D printing

A region of the cranial surface of the distal radius was marked, and the surface extruded 3 mm to form the guide base. The base included both osteotomy planes and extended distally to include the extensor groove approximately 5 mm from the carpal joint. For group 1 and 2 closing wedges, the osteotomy planes were converted to solid parts and extruded 1.5 mm thickness as

a shelf for the saw blade. Support struts were created using 3 mm diameter cylinders to join the proximal and distal osteotomy planes. For group 3, the single osteotomy plane was extruded to a thickness of 4 mm and then hollowed in the center to create a 1 mm slot for the saw blade. Two 1.1 mm diameter hollow cylinders with 1.5 mm wall thickness were created to secure the guide to the radius. All components listed above were joined into a single part and were exported as .STL files for 3D printing (Figure 2). Guides were printed on a stereolithographic (SLA) 3D printer (Form 2, Form Labs, Somerville, Massachusetts) using clear resin with a 50 micron resolution.

2.5 | Osteotomy

A standard craniomedial approach was made to the distal radius. Time was recorded from start of guide application or measurement of the FH wedge until osteotomy completion. For the limbs using 3D PSG, the guide was fitted to match the contours of the cranial of the distal radius, and secured to the bone with 1.1 mm Kirschner wires. For groups 1 and 2, the support struts were removed using an oscillating saw (25.5 mm × 0.38 mm blade, Stryker TPS, Kalamazoo, Michigan) before the osteotomies were performed. Osteotomies were performed by placing the saw blade flat against the shelf (wedge groups) or within the slot (SOO group). After completion of the osteotomies, the Kirschner wires and guides were removed. The wedge was preserved in the surgical field and sutured subcutaneously for postoperative imaging, and the skin was closed.

For the FH approach, the desired distance from the carpal joint was measured (25% of radial length) for the proximal transverse cut marked on the bone. The bone diameter was measured at this location using a sterile ruler. Trigonometric measurements for the desired wedge height were computed based on individual measured bone diameter. For example, a 30° wedge with bone diameter of 15 mm results in a 8.7 mm wedge height ($\tan 30^\circ \times 15 \text{ mm} = 8.7 \text{ mm}$). The wedge height and proposed osteotomy locations were marked using a pencil on the bone surface as appropriate for groups 1 and 2. The proximal and then distal osteotomies were completed with an observer assisting with saw blade orientation. The wedge was preserved and sutured subcutaneously and the skin was sutured. For the group 3 FH approach, a 0.045" reference pin was inserted from cranial to caudal on the cranial surface of the proximal radius to indicate the true sagittal plane using the palpation of the humeral epicondyles as an anatomic reference and an observer assisting with orientation. Angle measurements were calculated as

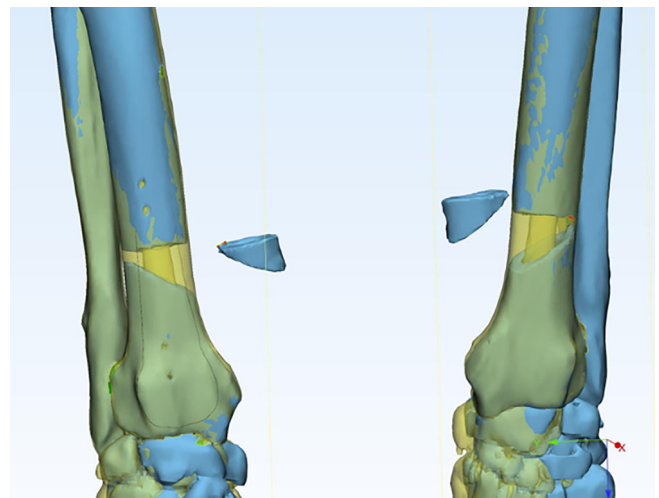


FIGURE 3 The preoperative (yellow) and postoperative (blue) limbs were shape matched using common points of reference and automated global registration.

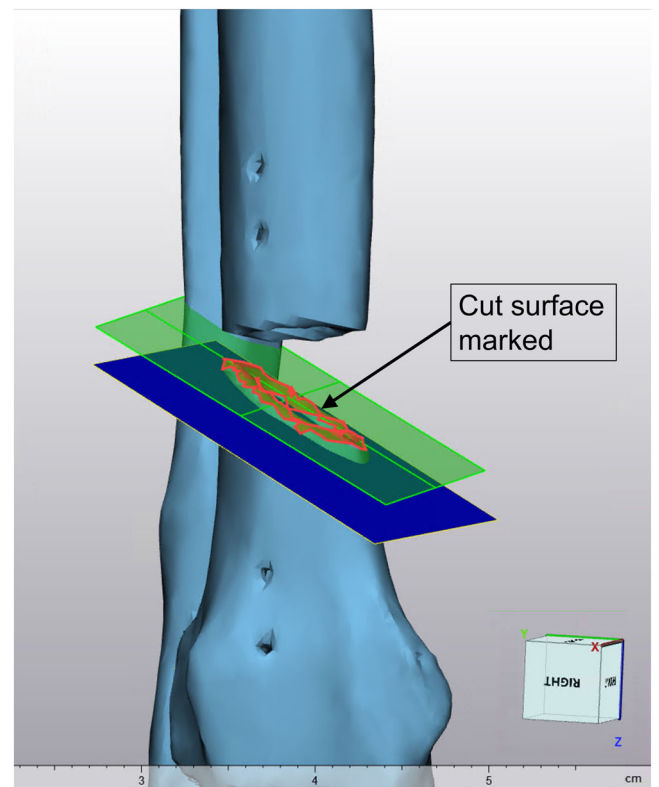


FIGURE 4 The intended target osteotomy (blue plane) as measured on the preoperative limb was compared to the achieved osteotomy plane (green plane) as measured with a fit plane to the marked surface of osteotomy on the postoperative limb.

described.¹² A sterile goniometer was used to measure 63.5° from cranial to medial in the transverse plane and a second pin was placed as a reference for the second measurement. A sterile goniometer was then used to measure

49° distal to align the blade to make a distomedial to proximal osteotomy. A thin piece of radiolucent gel was placed between the proximal and distal radial segments to separate them for postoperative CT scan. All limbs were frozen in extension postoperatively prior to scanning.

2.6 | Postoperative analysis

Computed tomography images of the postoperative limbs were obtained and 3D volumetric mesh reconstructions were made as described above. The proximal radius,

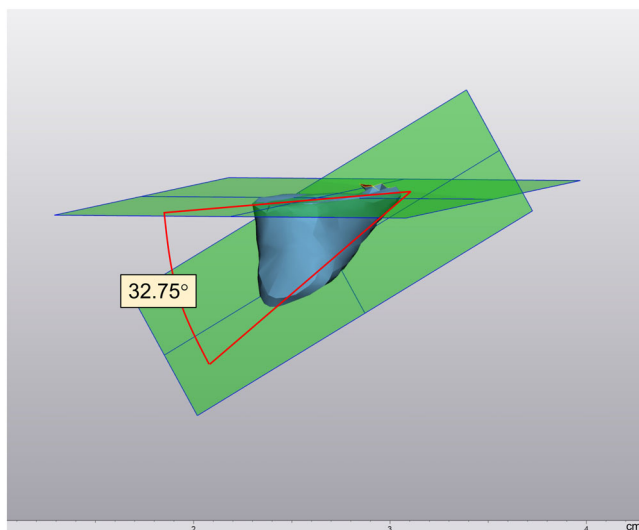


FIGURE 5 The wedges from groups 1 and 2 were measured and compared to their intended target wedge size. A plane was fit to each marked wedge cut surface and measured in 3-dimensions.

distal radius, and wedge were segmented and manually separated for assessment using 3D software. The preoperative and postoperative proximal and distal radius 3D meshes were shape matched to one another using four common prominent reference points on each segment (aspects of radial head, radial shaft, styloid, extensor groove) to approximate their overlay. An automated iterative process registration tool (global registration, 3-Matic) was then used to optimize the overlay between preoperative and postoperative radii (Figure 3). The actual osteotomy planes were defined by fitting a plane to marked surfaces of the postoperative bone proximally and distally. Similarly, a plane was fitted to the marked cut surface of the removed wedge (groups 1 and 2). The virtual target and actual osteotomy planes were compared (Figure 4). Deviance was measured separately in each frontal and sagittal plane using the previously defined object coordinate system as well as in 3D (combined *x*, *y*, and *z* planes). The actual wedge was compared to the target wedge size and their absolute difference was recorded (Figure 5). The actual single oblique plane osteotomy was measured relative to the target osteotomy using the proximal surface of the osteotomy plane and differences in the frontal, sagittal, and combined 3D planes were recorded as described above.

2.7 | Data analysis

Data were evaluated for normality using the Kolmogorov–Smirnov test and graphical visual assessment. Deviance from the virtual target osteotomy angle and location were determined for all osteotomies.

TABLE 1 Mean \pm standard deviation angle deviation for 3D-printed patient-specific guide compared to freehand corrective osteotomies in 32 normal ex vivo canine radii.

Group	Osteotomy location		3D PSG	FH	<i>p</i>
Frontal uniplanar wedge osteotomy	Proximal	Frontal	1.5 \pm 1.2*	5.7 \pm 1.4	<.001
		Sagittal	1.9 \pm 1.7	4.3 \pm 3.2	.096
	Distal	Frontal	1.5 \pm 1.7*	5.8 \pm 4.0	.006
		Sagittal	3.5 \pm 1.7	5.3 \pm 3.1	.161
	Wedge	3D	2.9 \pm 2.9	2.5 \pm 1.3	.061
Oblique plane wedge osteotomy	Proximal	Frontal	2.6 \pm 2.5	2.3 \pm 1.4	.705
		Sagittal	4.3 \pm 2.3	4.2 \pm 2.0	.944
	Distal	Frontal	1.6 \pm 1.3*	4.1 \pm 2.7	.037
		Sagittal	3.6 \pm 2.0	3.6 \pm 2.9	.955
	Wedge	3D	4.4 \pm 2.9	2.4 \pm 2.4	.563
Single oblique plane osteotomy	Frontal		5.3 \pm 4.1*	17.8 \pm 6.0	.002
	Sagittal		2.1 \pm 1.1*	10.5 \pm 9.6	.043

Abbreviations: FH, freehand; PSG, patient-specific guide. **C p* < .05.

Accuracy and time using 3D PSG was compared to a FH approach in each osteotomy group separately using a paired *t*-test. A clinically relevant threshold of within 5° of target was established as a cut point. Frequencies of clinically acceptable angles were compared between approaches using McNemar's test for paired proportions. Statistical analysis was performed using commercial software (R, version 3.0, Development Core Team, Vienna, Austria). All comparisons were considered significant at $p < .05$.

3 | RESULTS

For group 1 (single frontal plane closing wedge), the frontal plane deviation was increased in the FH limbs in comparison with the 3D PSG limbs on the proximal, transverse ($p < .001$) and the distal osteotomy ($p = .006$) (Table 1). The sagittal plane deviation was not different

for either proximal or distal osteotomy. The actual wedge angle (30°) was not different between 3D PSG and FH groups.

In group 2 (oblique plane closing wedge), the frontal plane deviation of the distal osteotomy was increased in FH limbs compared to 3D PSG ($p = .037$). No other osteotomy or wedge measurements were different between groups (Table 1).

In Group 3 (SOO), the FH osteotomy deviance was increased in comparison with the 3D PSG osteotomy in the frontal ($p = .002$) and sagittal planes ($p = .043$).

The combined deviance in 3D (x, y, z planes) was not different for groups 1 and 2. The 3D deviance for group 3 was increased in the FH osteotomy group relative to the 3D PSG ($p = .001$).

Overall, 3D PSG osteotomies were closer to the target osteotomy using a 5° clinically acceptable threshold for accuracy in ALD correction. In groups 1 and 2, 32 total measurements were obtained in individual

TABLE 2 Frequency of corrective osteotomies excess of 5° tolerance of the intended virtual target.

Group	Osteotomy type		3D PSG	FH	<i>p</i> value
Frontal uniplanar osteotomy	Proximal	Frontal	0%	75%*	.041
		Sagittal	13%	50%	.371
	Distal	Frontal	0%	63%	.074
		Sagittal	25%	63%	.248
	Pooled (n = 32 osteotomies)		9%	63%*	<.001
3D Wedge	(x, y, z)	0%	25%	.467	
Oblique plane osteotomy	Proximal	Frontal	13%	0%	.999
		Sagittal	38%	50%	.999
	Distal	Frontal	0%	38%	.248
		Sagittal	25%	13%	.999
	Pooled (n = 32 osteotomies)		19%	25%	.724
3D Wedge	(x, y, z)	13%	38%	.467	
Single oblique plane osteotomy		Frontal	50%	100%	.134
		Sagittal	0%	50%	.134
	Pooled (n = 16 osteotomies)		25%	75%*	.013

Abbreviations: PSG, patient-specific guide; FH, freehand. * $p < .05$.

TABLE 3 Mean \pm standard deviation distance deviation (mm) from target osteotomy location.

	3D PSG	FH
Group 1	1.0 \pm 0.9	1.9 \pm 1.2
Group 2	2.2 \pm 1.6	1.6 \pm 2.2
Group 3	2.9 \pm 1.3	2.2 \pm 1.3

Abbreviations: PSG, patient-specific guide; FH, freehand. * $p < .05$.

TABLE 4 Mean (\pm SD) time (s) to complete 3D PSG and FH osteotomies.

	3D PSG	FH
Group 1	358 \pm 43	372 \pm 81
Group 2	292 \pm 48	293 \pm 82
Group 3	84 \pm 10	162 \pm 35*

Abbreviations: PSG, patient-specific guide; FH, freehand. * $p < .05$.

planes (proximal/distal sagittal/frontal for 8 limb pairs). In group 1, 63% (20/32) of measurements were greater than 5° from the target osteotomy in the FH group, in comparison with 9% (3/32) in the 3D PSG group ($p < .001$). In group 2, 25% (8/32) of the FH measurements were greater than 5°, in comparison with 19% (6/32) of the 3D PSG measurements ($p = .72$). Group 3 had 16 measurements total in which 75% (12/16) of the FH group were greater than 5° from target, compared with 25% (4/16) of the 3D PSG measurements ($p = .013$) (Table 2).

The mean deviation of osteotomy location was less than 3 mm from the target location in all three osteotomy groups and was not different between the 3D PSG or FH approaches (Table 3). The maximum error across all groups was 5.5 mm and 6.8 mm using 3D PSG and FH approaches, respectively.

The time required to perform group 1 and 2 wedge osteotomies using the 3D PSG approach did not differ from the FH osteotomies (Table 4). The maximum times required in group 1 and group 2 were 346 and 489 seconds, respectively. Time to perform group 3 osteotomies (SOO) using 3D PSGs was less than for FH osteotomies ($p < .001$), and the maximum time was 106 and 226 seconds.

4 | DISCUSSION

The aim of the current study was to compare the accuracy of radial osteotomies performed using 3D PSGs versus the previous standard FH approach in normal ex vivo canine radii. It was hypothesized that 3D guide use would improve osteotomy angle and location accuracy. This hypothesis was partially supported for the simple frontal plane wedge and the most complex single oblique (inclined) plane osteotomy but not for oblique plane osteotomies. Using an acceptable osteotomy angle tolerance of 5°,³ it was found that 84% of 3DP guided osteotomies were within this range, in comparison of 50% of FH osteotomies.

Three-dimensional printed guides provided improved angle accuracy but this comparison with freehand was no different in the sagittal plane for both wedge groups. Guided osteotomy accuracy was consistent in all planes and typically within 5° of the targets. This is consistent with recent clinical case series of guided radial osteotomies in dogs with deformity.³ Freehand performance was more variable, with greater accuracy in group 2 as a whole and in the sagittal plane for groups 1 and 2. Intraoperative clinical assessment and alignment of a saw to this plane may be easier to execute although this has not been investigated specifically. Improvement in freehand

performance may also be related to increasing surgeon skill with sequential performance of the osteotomies (group 1, group 2, group 3). All osteotomies were performed by a surgical resident under the guidance of a board-certified surgeon. The resident had no prior clinical experience with corrective osteotomies other than completion of a practice osteotomy session on 2 limb pairs prior to this project. Right and left limbs were randomized for treatment but we could have considered randomizing group order too. Furthermore, the same individual who performed the 3D virtual planning and guide design conducted the subsequent surgical osteotomies. This preoperative planning process likely improved the outcomes overall but in particular for the freehand group. Despite these comments, improvement was not sustained in group 3; however, freehand orientation and execution of a single oblique plane osteotomy is considered very technically challenging.^{12,13}

Causes for deviation from the virtual target may vary between groups. The location of the osteotomy was generally accurate in all groups, typically within 3 mm. There was greater variation in the angles of the osteotomy planes. We did not account for the kerf of the saw blade (0.3 mm) during the assessment, which may have a small effect on our data. In 3D-guided cases, error may arise from imprecise guide placement on the bone, surgeon technical error such as bending of the oscillating saw blade away from guide shelves or slot, or flex of the guide material. In FH cases, surgeon technical error in measurements on the bone, or angle of the saw blade are potential sources of deviance.

The methods developed and used for limb alignment planes and postoperative analysis were novel and completed using 3D planning software. The frontal, sagittal, and axial planes of the proximal limb were based on a subjective visual assessment of the proximal antebrachium/distal humerus.^{3,8} Target osteotomy planes were measured in relation to these neutral planes on both the virtual and freehand corrections. Postoperative CT scans were individually shape-matched to the preoperative proximal limb using an automated iterative global 3D surface superimposition tool (global registration, 3-Matic). This is an established strategy for overlay of images and differential assessment with a precision of <0.5 mm depending on points or surface structure.¹⁴ This approach allowed for the direct comparison of the location and angle of the executed osteotomy and wedge to the intended virtual target. This strategy can be explored for use in clinical cases to precisely examine outcomes in three dimensions.

The time required for osteotomy execution after freehand templating or guide placement was evaluated in this study although the clinical relevance is limited with

normal dog cadaver limbs. Times were typically between 4 and 5 min for wedges and 1–2 minutes for the single oblique plane osteotomy. Freehand single oblique plane osteotomies took twice as long as 3D guided but a difference of 1 minute in the overall duration of a deformity correction is negligible. The time for osteotomy execution and corrected alignment in limbs with deformity may provide more clinically relevant comparisons. Subjectively, the guides were easy to apply to the distal radius. The use of the extensor groove as a unique anatomic landmark for guide contouring and placement instilled confidence in the novice resident surgeon. Execution of the FH osteotomies was more challenging in group 1, but confidence and efficiency increased as would be expected with repeated osteotomy performance.

Computed tomography-based 3D planning and additive manufacturing of 3D PSGs is now feasible, efficient, and cost effective.^{11,15,16} Orthopedics and bone deformities are a natural target due to ease of automated threshold-based segmentation of bone and the technical challenge of assessment and successful correction of complex cases. The 3D-PSGs offer an operative tool to take a complex alignment assessment (degrees of difference in three planes) and ensure accuracy in intraoperative execution. Guides provide both novice and experienced surgeons added comfort in the execution of a technique but does not replace good surgical acumen. Guides are typically built with a base contoured to the normal anatomy that creates a key-in-lock fit of the guide onto the bone, which is essential to achieve the intended target. Outcomes and operative time saved may outweigh time and resources required for 3D planning and manufacturing of guides, although this analysis has not been explored.

The authors have experienced a paradigm shift in their practices having collectively performed hundreds of deformity corrections FH, prior to a change in the past 5–10 years performing nearly all clinical cases using 3D PSG osteotomy and alignment guides. Anecdotally, the ease of guide application, lack of intraoperative subjectivity, and reduction of surgical time are dramatic improvements with current 3D PSG. More objective data to support these observations and comparisons in affected deformity cases are targets of future work.

Limitations of this study include use of normal *ex vivo* dog limbs. Subjective freehand alignment assessment in limbs with bone deformity is more challenging, which may have led to greater differences in comparison with guide use. We only evaluated osteotomy execution as we did not feel reduction of bone ends into a malaligned orientation would be clinically relevant. In the authors' experience, 3DP alignment guides provided an

even greater benefit than osteotomy guides in achieving optimal clinical outcomes.

Our data would suggest that as the complexity of the desired osteotomy increases, the guides become more critical. The use of guides resulted in more consistent acceptable outcomes across all osteotomy types. The advanced 3D methods used for limb alignment and 3D outcome assessment may be useful and improve clinical assessments. Future work evaluating 3D PSG in limbs with deformities may provide additional guidance to refine clinical case selection more effectively.

ACKNOWLEDGMENTS

Author Contributions: Townsend A, DVM: Study design, data acquisition, manuscript preparation. Guevar J, DVM, MVM, DECVN, MRCVS: Study design, manuscript preparation. Oxley B, MA, VetMB, DSAS(Orth): Study design, manuscript preparation. Hetzel S, MS: Statistical analysis, manuscript preparation. Bleedorn J, DVM, MS, DACVS-SA: Study conception, data acquisition, manuscript preparation.

The authors would like to thank Dr Sun Young Kim of Purdue University for his assistance and expertise in the single oblique osteotomy.

CONFLICT OF INTEREST STATEMENT

Bill Oxley is the founder and owner of Vet3D. The authors declare no other conflicts of interest or financial interests related to this report.

ORCID

Jason Bleedorn  <https://orcid.org/0000-0003-2987-7722>

REFERENCES

- Knapp JL, Tomlinson JL, Fox DB. Classification of angular limb deformities affecting the canine radius and ulna using the Center of Rotation of angulation method. *Vet Surg*. 2016;45:295-302.
- Fox D, Tomlinson J, Cook JL, et al. Principles of Uniapical and Biapical radial deformity correction using dome osteotomies and the Center of Rotation of angulation methodology in dogs. *Vet Surg*. 2006;35:67-77.
- De Armond CC, Lewis DD, Kim SE, Biedrzycki AH. Accuracy of virtual surgical planning and custom three-dimensionally printed osteotomy and reduction guides for acute uni- and biapical correction of antebrachial deformities in dogs. *J Am Vet Med Assoc*. 2022;22:1-9.
- Cooley K, Kroner K, Muir P, Hetzel SJ, Bleedorn JA. Assessment of overall thoracic limb axial alignment in dogs with antebrachial deformity. *Vet Surg*. 2018;47:1074-1079.
- Aimar A, Palermo A, Innocenti B. The role of 3D printing in medical applications: a state of the art. *J Healthc Eng*. 2019;2019:5340616-5340610.
- Hall EL, Baines S, Bilmont A, Oxley B. Accuracy of patient-specific three-dimensional-printed osteotomy and reduction

- guides for distal femoral osteotomy in dogs with medial patella luxation. *Vet Surg.* 2019;48:584-591.
7. Dismukes DI, Fox DB, Tomlinson JL, Essman SC. Use of radiographic measures and three-dimensional computed tomographic imaging in surgical correction of an antebrachial deformity in a dog. *J Am Vet Med Assoc.* 2008;232:68-73.
 8. Carwardine DR, Gosling MJ, Burton NJ, O'Malley FL, Parsons KJ. Three-dimensional-printed patient-specific osteotomy guides, repositioning guides and titanium plates for acute correction of antebrachial limb deformities in dogs. *Vet Comp Orthop Traumatol.* 2021;34:43-52.
 9. Elford JH, Oxley B, Behr S. Accuracy of placement of pedicle screws in the thoracolumbar spine of dogs with spinal deformities with three-dimensionally printed patient-specific drill guides. *Vet Surg.* 2019;9:347-353.
 10. Winer JN, Verstraete FJM, Cissell DD, Lucero S, Athanasiou KA, Arzi B. The application of 3-dimensional printing for preoperative planning in oral and maxillofacial surgery in dogs and cats. *Vet Surg.* 2017;46:942-951.
 11. Guiot LP, Allen MJ. Three-dimensional printing: building a solid foundation for improving technical accuracy in orthopaedic surgery. *Vet Comp Orthop Traumatol.* 2021;34:v-vi.
 12. Kim SY, Snowdon KA, DeCamp CE. Single oblique osteotomy for correction of antebrachial angular and torsional deformities in a dog. *J Am Vet Med Assoc.* 2017;251:333-339.
 13. Franklin SP, Dover RK, Andrade N, Rosselli D, Clarke KM. Correction of antebrachial angulation-rotation deformities in dogs with oblique plane inclined osteotomies. *Vet Surg.* 2017;46:1078-1085.
 14. Gkantidis N, Schauseil M, Pazera P, Zorkun B, Katsaros C, Ludwig B. Evaluation of 3-dimensional superimposition techniques on various skeletal structures of the head using surface models. *PLoS One.* 2015;10:e0118810.
 15. Harrysson OLA, Marcellin-little, DJ & Horn, TJ applications of metal additive manufacturing in veterinary orthopedic surgery. *JOM.* 2015;67:647-654.
 16. Altwal J, Wilson CH, Griffon DJ. Applications of 3-dimensional printing in small-animal surgery: a review of current practices. *Vet Surg.* 2022;51:34-51.

How to cite this article: Townsend A, Guevar J, Oxley B, Hetzel S, Bleedorn J. Comparison of three-dimensional printed patient-specific guides versus freehand approach for radial osteotomies in normal dogs: Ex vivo model. *Veterinary Surgery.* 2023;1-9. doi:10.1111/vsu.13968